DATA-DRIVEN ROBUST OPTIMAL ITERATIVE LEARNING CONTROL OF LINEAR SYSTEMS WITH STRONG CROSS-AXIS COUPLING¹

Zezhou Zhang², Qingze Zou²

Abstract—In this paper, a data-driven iterative learning control approach to multi-input-multi-output (MIMO) systems with strong cross-axis coupling is proposed. Iterative learning control (ILC) of MIMO systems with strong cross-axis coupling effect is challenging as model-based ILC to MIMO systems is complicated by the modeling process of MIMO systems being involved and time-consuming, the trade-off between the model accuracy and the performance, and the limitation to systems with weak-cross-coupling. Contrarily, constant gain ILC methods are mainly effective for tracking at low-speed, and suffer from slow convergence, particularly in the presence of the random disturbances. Thus, the aim of this paper is to develop a data-driven robust optimal ILC (DDRO-ILC) approach to MIMO systems of strong cross-axis coupling under random output disturbance. The iteration gain is constructed and updated by using past input and output data to capture the dynamics of the system via the singular value decomposition (SVD) technique. It is shown that monotonic convergence in the presence of random disturbance is guaranteed, and an optimal gain can be obtained to maximize the convergence rate and minimize the residual error. The proposed DDRO-ILC technique is illustrated through a numerical simulation on a three-input three-output linear time invariant system model, and compared to the multi-axis inversion-based iterative control (MAIIC) technique. The simulation shows that the proposed DDRO-ILC outperformed the MAIIC method when the crossaxis coupling is strong, and achieved precision tacking with rapid convergence in the presence of random disturbance.

I. INTRODUCTION

In this paper, a data-driven robust optimal iterative learning control technique is proposed for output tracking of multiinput multi-output (MIMO) systems under random output disturbance. Precision tracking of MIMO systems plays a significant role in various applications, ranging from manufacturing process [1], atomic force microscope (AFM) [2], robotics systems [3], [4], industrial printer [5] to wafer stage positioning [6]. In these applications, the output tracking is characterized by periodic motion, and thereby, iterative learning control (ILC) becomes a natural choice to achieve multi-axis precision tracking [1], [7]. However, existing ILC techniques are challenged by issues arising from crosscoupling dynamics, random noise disturbances, and trade-off between robustness and tracking performance. These issues are tackled through the development of the proposed DDRO-ILC technique in this work.

Limitations exist in current ILC techniques for highspeed precision tracking of general MIMO systems. For example, PID type of ILC algorithms [8], [9] have been proposed for MIMO systems under mechanical vibrations or initial position offset. This relatively simple ILC method, however, is slow in convergence (e.g., over 200 iterations in [8]), and the working bandwidth is low, resulting in poor performance in high-speed tracking. The working bandwidth can be increased by using system dynamics model in the ILC technique to optimize the ILC controller [10]. Although both the tracking performance and the convergence rate are improved, the design of the robustness filter is complicated, and accurate parameterized model of the system dynamics is needed, whereas the modeling process is time-consuming and prone to uncertainties and variations in practice. The tracking performance can be further enhanced through the inversion-based ILC approach [11]. The performance, however, can be sensitive to the accuracy of the system inversion and thereby, the modeling process [12]. Moreover, additional approximation error is induced for non-square systems, and the tracking performance is limited for non-minimum phase systems. The complexity of modeling MIMO systems can be alleviated by ignoring the cross-axis coupling dynamics and using only the dynamics model of the diagonal sub-systems in the inversion-based ILC control law [2]. The algorithm converges rapidly, and the tracking performance at highspeed is largely improved. However, dynamics modeling process is still needed, and the cross-coupling dynamics needs to be relatively small (i.e., the combined cross-couple dynamics needs to be smaller than the diagonal dynamic [2]). The pseudoinverse-based iterative learning control has been explored for nonlinear, nonminimum-phase plants via linearization [13]. However, a precise model of the system is still needed and the performance depends on the quality of the linearization itself. Therefore, further development in ILC is needed to simplify or even avoid the modeling process, and account for the strong cross-coupling dynamics efficiently.

Recent development in data-driven ILC approaches provides an effective avenue to address these issues related to dynamics modeling and strong-cross dynamics. Unlike those parameterized-model-based ILCs, data-driven ILCs directly utilize the input and output data acquired in past iterations to update the iterative control input. As such, the modeling process is avoided, and both the performance and the robustness of the ILC technique are improved. For example, a data-driven ILC approach [14] has been proposed to mitigate

¹This work was supported by NSF CMMI-1851907 and IIBR-1952823. ²The authors are with the Department of Mechanical and Aerospace Engineering, Rutgers University, Piscataway, NJ, 08854, USA (e-mail: zezhou.zhang@rutgers.edu; qzzou@soe.rutgers.edu).

the performance/robustness trade-off without modeling the system dynamics, where the concept of Hessian information has been explored to increase the convergence rate. The design of the weighting matrices, however, depends on a priori expertise knowledge of the system gained from a large number of experiments. Such a requirement of expertise knowledge can be alleviated through a data-driven gradientbased ILC method [15], where an explicit model of the plant is not required. Instead, additional experiment is need between each ILC trial, resulting in extra effort from user, and the robustness performance is not systematically considered. The number of experiments needed can be reduced through a stochastic-based data-driven ILC technique [16]. However, only is the convergence of the error expectation considered, the variation of the tracking error is not characterized, and the iteration coefficient needs to be carefully tuned, resulting in a conservative performance and slow convergence rate (e.g., over a hundred of iterations are needed in [16]). Therefore, how to achieve both rapid convergence and robust performance in the presence of general cross-axis coupling effect remains as a challenge in data-driven MIMO ILCs.

The main contribution of this paper is the development of a data-driven robust optimal iterative learning control (DDRO-ILC) method for MIMO systems. Specifically, tracking of trajectories with a finite discrete spectrum (i.e., sparse spectrum) is considered. After the initialization, the input and output data obtained in past iterations are used to approximate the system inverse in the iteration gain via the SVD technique. We show that in the presence of random output disturbance/noise, monotonic convergence is achieved, and the converged tracking error is bounded by a class κ function of the disturbance size. Moreover, an optimal gain is designed to maximize the convergence rate and minimize the tracking error against the random disturbance. The performance of the proposed method over the MAIIC method [2] is demonstrated through a simulation study on 3-axis output tracking example.

II. PROBLEM FORMULATION

Consider a square MIMO LTI system given in the frequency domain

$$\mathbf{y}_k(j\omega) = \mathbf{G}(j\omega)\mathbf{u}_k(j\omega) + \mathbf{d}_k(j\omega), \tag{1}$$

where ' $j\omega$ ' denotes the Fourier transform of a time-domain signal, $G(j\omega) \in \mathbb{C}^{p \times p}$ is the transfer function matrix [17] and for each k^{th} iteration, $y_k(j\omega) \in \mathbb{C}^{p \times 1}$, $u_k(j\omega) \in \mathbb{C}^{p \times 1}$, $d_k(j\omega) \in \mathbb{C}^{p \times 1}$ are the input and output of the system, and the output disturbance (e.g., measurement noise), respectively.

In general, a linear ILC algorithm can be represented as: $u_{k+1}(j\omega) = q_k(j\omega)u_k(j\omega) + l_k(\omega)e_k(j\omega), \ k \ge 1$, (2) where $q_k(j\omega) \in \mathbb{C}^{p \times p}$ is usually a low-pass filter (to improve the robustness against noise/disturbance), and $l_k(\omega) \in \mathbb{C}^{p \times p}$ is a frequency- and iteration- dependent iteration gain matrix to be designed (to ensure the convergence of the ILC algorithm). Moreover, we assume that

Assumption 1. The desired trajectory in the i^{th} output channel contains a finite N_i number of frequencies, i.e.,

for any given $i=1,2\cdots p$, the desired trajectory of any i^{th} output channel, $y_{i,d}(j\omega)=0$, except at $\omega=\omega_{s,i}$ for $s=1,2,\cdots,N_i$.

In practice, tracking becomes infeasible when the amplitude of a given frequency component is too small—smaller than the size of the random noise. Thus, we define

Definition 1 (Active Frequency). For any given constant $\epsilon_Y > 0$, $\omega_{s,t}$ for any $t = 1, 2, \dots, p$, and any $s = 1, 2 \dots, N_t$ is called the s^{th} active frequency of the t^{th} channel if the amplitude of the corresponding desired output satisfies $|y_{t,d}(j\omega_{s,t})| \ge \epsilon_Y$, and $\mathbb{S}_a := \bigcup_t \mathbb{S}_{a,t}$ is the set of active frequencies.

In the following, we order the active frequencies in \mathbb{S}_a in the ascending order, i.e., $\omega_1 \leq \cdots \omega_{N_q}$, with $N_q = |\mathbb{S}_a|$. Assumption 2. The transfer function matrix, $G(j\omega)$, is proper, stable, and hyperbolic, i.e., for any $i,j \in \mathbb{N}^*$ (\mathbb{N} : the set of the natural numbers), the corresponding transfer function, $g_{i,j}(j\omega) \in G(j\omega)$, is proper, stable and hyperbolic. We also assume that transmission zeros [18] of the system, $z_i \in \mathbb{C}$ $(i \in \mathbb{N})$, do not overlap with the active frequency. i.e., $z_i \notin \mathbb{S}_a$ for all i.

First, we format the input and output trajectory matrices needed in the proposed DDRO-ILC technique. For any given r^{th} input-output channel $(r=1,2,\cdots p)$: let the active desired trajectory matrix, $\mathbf{Y}_{r,d}(\mathbb{S}_a) \in \mathbb{C}^{N_q \times N_q}$ $(1 \leq r \leq p)$, the active input and output matrix in the k^{th} iteration, $\mathbf{U}_{r,k}(\mathbb{S}_a) \in \mathbb{C}^{N_q \times N_q}$ $(1 \leq r \leq p)$ and $\mathbf{Y}_{r,k}(\mathbb{S}_a) \in \mathbb{C}^{N_q \times N_q}$ $(1 \leq r \leq p)$, respectively, be given by:

$$\begin{aligned} & \boldsymbol{Y}_{r,d}(\mathbb{S}_a) = \operatorname{diag}([y_{r,d}(j\omega_1) \ \cdots \ y_{r,d}(j\omega_{N_q})])_{N_q \times N_q}, \\ & \boldsymbol{Y}_{r,k}(\mathbb{S}_a) = \operatorname{diag}([y_{r,k}(j\omega_1) \ \cdots \ y_{r,k}(j\omega_{N_q})])_{N_q \times N_q}, \end{aligned} \tag{3} \\ & \boldsymbol{U}_{r,k}(\mathbb{S}_a) = \operatorname{diag}([u_{r,k}(j\omega_1) \ \cdots \ u_{r,k}(j\omega_{N_q})])_{N_q \times N_q}, \end{aligned}$$

where diag{[V]} denotes a diagonal matrix with the diagonal entries given by the vector $V = [v_1 \ v_2 \ \cdots \ v_{N_q}]$. Then, the active output tracking error matrix, $E_k(\mathbb{S}_a)$, is given by

$$\boldsymbol{E}_k(\mathbb{S}_a) = \boldsymbol{Y}_d(\mathbb{S}_a) - \boldsymbol{Y}_k(\mathbb{S}_a), \quad \text{where}$$

$$\mathbf{Y}_{k}(\mathbb{S}_{a}) = \begin{bmatrix} \mathbf{Y}_{1,k}(\mathbb{S}_{a}) & \cdots & \mathbf{Y}_{p,k}(\mathbb{S}_{a}) \end{bmatrix}_{pN_{q} \times N_{q}}^{T}, \quad k \geq 0,$$
(4)

Then, the active input matrix $U_k(\mathbb{S}_a)$ can be represented in $U_{i,k}(\mathbb{S}_a)(1 \leq i \leq p)$ similarly as how the active output matrix $Y_k(\mathbb{S}_a)$ is represented in $Y_{i,k}(\mathbb{S}_a)(1 \leq i \leq p)$ as in the above Eq. (4).

Thus, the general ILC algorithm Eq. (2) can also be written in terms of the active set \mathbb{S}_a as

$$U_{k+1}(\mathbb{S}_a) = \mathcal{Q}_k(\mathbb{S}_a)U_k(\mathbb{S}_a) + L_k(\mathbb{S}_a)E_k(\mathbb{S}_a), \ k \ge 1, \ (5)$$

where $Q_k(\mathbb{S}_a)$, $L_k(\mathbb{S}_a) \in \mathbb{C}^{pN_q \times pN_q}$ are the corresponding active low-pass filter and active iteration gain matrix. In this article, we consider $Q_k(\mathbb{S}_a) = I$ (I: Identity matrix of the same dimension) and focus on the design of $L_k(\mathbb{S}_a)$.

DATA-DRIVEN ROBUST OPTIMAL ITERATIVE LEARNING CONTROL (DDRO-ILC) OF LTI SYSTEM PROBLEM For a LTI system given in Eq. (1), let Assumptions 1 and 2 be hold, then the DDRO-ILC is to design the active iterative learning gain matrix $L_k(\mathbb{S}_a)$ such that:

- \mathcal{O}_1 The active iteration gain matrix, $L_k(\mathbb{S}_a)$, is constructed and updated in each iteration using only the measured input-output data.
- \mathcal{O}_2 Unbiased and monotonic convergence is guaranteed in the sense that for each k^{th} iteration, the active output tracking error is monotomically decreasing $\|\boldsymbol{E}_k(\tilde{\mathbb{S}_a})\|_2 < \|\boldsymbol{E}_{k-1}(\mathbb{S}_a)\|_2, \quad \lim_{k \to \infty} ||\boldsymbol{E}_k(\tilde{\mathbb{S}_a})||_2 \le \mathcal{L}(\varepsilon_n),$ where $||v||_2$ denotes 2-norm of the vetor v, and $\mathcal{L}(\cdot)$: $\mathbb{R}^* \to \mathbb{R}^*$ is a class κ function of ε_n [19] and thereby $\lim_{\varepsilon_n \to 0} \mathcal{L}(\varepsilon_n) = 0.$
- \mathcal{O}_3 Optimize the active iteration gain matrix, $L_k(\mathbb{S}_a)$, in the sense that the upper bound of the tracking error is minimized, and the convergence speed is maximized in terms of the upper bound of the tracking error, i.e., find $L_{k}^{*}(\mathbb{S}_{a})$, such that for any given active frequency $\omega_a \in \mathbb{S}_a$ and any given iteration k,

$$\min_{\boldsymbol{L}_{k}(\mathbb{S}_{a})} \frac{\|\boldsymbol{E}_{k}(\mathbb{S}_{a})\|_{2}, \quad \text{and} \\
\max_{\boldsymbol{L}_{k}(\mathbb{S}_{a})} \left| \overline{\|\boldsymbol{E}_{k}(\mathbb{S}_{a})\|_{2}} - \overline{\|\boldsymbol{E}_{k-1}(\mathbb{S}_{a})\|_{2}} \right|$$
(7)

are achieved, where $\overline{\|E_k(\mathbb{S}_a)\|_2}$ is the upper bound of $||E_k(\mathbb{S}_a)||_2$.

III. DATA-DRIVEN ROBUST ITERATIVE LEARNING CONTROL METHOD OF MIMO **SYSTEM**

In this section, we present the proposed DDRO-ILC technique by achieving the above three objectives. We start with constructing the active iteration gain matrix $L_k(\mathbb{S}_a)$ by using the past input-output data only (Objective \mathcal{O}_1).

A. DDRO-ILC ALGORITHM

The proposed DDRO-ILC algorithm is:

$$\begin{aligned} & \boldsymbol{U}_{1}(\mathbb{S}_{a}) = \mathbb{U}_{int}(\mathbb{S}_{a})\mathbb{Y}_{int}^{\dagger}(\mathbb{S}_{a})\boldsymbol{Y}_{d}(\mathbb{S}_{a}), & k = 1, \\ & \boldsymbol{U}_{k}(\mathbb{S}_{a}) = \boldsymbol{U}_{k-1}(\mathbb{S}_{a}) + \Delta\mathbb{U}_{k-1,s}(\mathbb{S}_{a})\Delta\mathbb{Y}_{k-1,s}^{\dagger}(\mathbb{S}_{a})\boldsymbol{\Phi}_{k-1}(\mathbb{S}_{a}) \\ & \boldsymbol{E}_{k-1}(\mathbb{S}_{a}), & k \geq 2, \\ & (8) \end{aligned}$$

where $\{\mathbb{U}_{int}(\mathbb{S}_a)\}_{pN_q\times pN_q}$ and $\{\mathbb{Y}_{int}(\mathbb{S}_a)\}_{pN_q\times pN_q}$ are the active initialization input and output matrix, respectively:

$$\mathbb{U}_{int}(\mathbb{S}_a) = \begin{bmatrix} \tilde{U}_{int,1}(\mathbb{S}_a) & \cdots & U_{int,p}(\mathbb{S}_a) \end{bmatrix},
\mathbb{Y}_{int}(\mathbb{S}_a) = \begin{bmatrix} \mathbf{Y}_{int,1}(\mathbb{S}_a) & \cdots & \mathbf{Y}_{int,p}(\mathbb{S}_a) \end{bmatrix},$$
(9)

 $\mathbb{Y}_{int}(\mathbb{S}_a) = \begin{bmatrix} \mathbf{Y}_{int,1}(\mathbb{S}_a) & \cdots & \mathbf{Y}_{int,p}(\mathbb{S}_a) \end{bmatrix},$ with $\{\mathbf{U}_{int,i}(\mathbb{S}_a)\}_{pN_q \times N_q}$ and $\{\mathbf{Y}_{int,i}(\mathbb{S}_a)\}_{pN_q \times N_q}$ are the so-called i^{th} active initialization input and the corresponding output matrix (specified immediately below in Sec. III-B), respectively. In Eq. (8),

Espectively. In Eq. (6),

$$\Delta \mathbb{U}_{k,s}(\mathbb{S}_a) = \begin{bmatrix} \mathbb{U}_{int}(\mathbb{S}_a) & \Delta U_k(\mathbb{S}_a) \end{bmatrix}_{pN_q \times ((p+1)N_q)},$$

$$\Delta \mathbb{Y}_{k,s}(\mathbb{S}_a) = \begin{bmatrix} \mathbb{Y}_{int}(\mathbb{S}_a) & \Delta Y_k(\mathbb{S}_a) \end{bmatrix}_{pN_q \times ((p+1)N_q)},$$
(10)

$$\Delta \boldsymbol{U}_{k}(\mathbb{S}_{a}) = \begin{cases} \boldsymbol{U}_{1}(\mathbb{S}_{a}) - \boldsymbol{U}_{int,p+1}(\mathbb{S}_{a}), & \text{when } k = 1\\ \boldsymbol{U}_{k}(\mathbb{S}_{a}) - \boldsymbol{U}_{k-1}(\mathbb{S}_{a}), & \text{when } k \geq 2 \end{cases},$$

$$\Delta \boldsymbol{Y}_{k}(\mathbb{S}_{a}) = \begin{cases} \boldsymbol{Y}_{1}(\mathbb{S}_{a}) - \boldsymbol{Y}_{int,p+1}(\mathbb{S}_{a}), & \text{when } k = 1\\ \boldsymbol{Y}_{k}(\mathbb{S}_{a}) - \boldsymbol{Y}_{k-1}(\mathbb{S}_{a}), & \text{when } k \geq 2 \end{cases}.$$

Finally, $\Delta \mathbb{Y}_{k,s}^{\dagger}(\mathbb{S}_a)$ in Eq. (9), denotes the Moore-Penrose pseudoinverse of $\Delta \mathbb{Y}_{k,s}(\mathbb{S}_a)$, and $\Phi_k(\mathbb{S}_a) \in \mathbb{C}^{pN_q \times pN_q}$ is the iteration gain matrix.

Comparing Eq. (8) to Eq. (2) shows that in the proposed DDRO-ILC algorithm, the active iteration gain matrix $L_k(\mathbb{S}_a)$ is given by

$$\mathbf{L}_{k}(\mathbb{S}_{a}) = \Delta \mathbb{U}_{k,s}(\mathbb{S}_{a}) \Delta \mathbb{Y}_{k,s}^{\dagger}(\mathbb{S}_{a}) \mathbf{\Phi}_{k}(\mathbb{S}_{a}). \tag{12}$$

Thus, $L_k(\mathbb{S}_a)$ is data-driven if the gain matrix $\Phi_k(\mathbb{S}_a)$ is determined by past input-output data. This can be obtained by computing the Moore-Penrose pseudoinverse of $\Delta \mathbb{Y}_{k,s}(\mathbb{S}_a)$ via the Singular Value Decomposition (SVD) [20] of $\Delta \mathbb{Y}_{k,s}(\mathbb{S}_a)$:

$$\Delta \mathbb{Y}_{k,s}(\mathbb{S}_{a}) = \mathcal{U}_{k}(\mathbb{S}_{a}) \Sigma_{k}(\mathbb{S}_{a}) V_{k}^{H}(\mathbb{S}_{a})
= \begin{bmatrix} \mathcal{U}_{1,k}(\mathbb{S}_{a}) & \mathcal{U}_{2,k}(\mathbb{S}_{a}) \end{bmatrix}
\begin{bmatrix} \Sigma_{1,k}(\mathbb{S}_{a}) & \mathbf{0} \\ \mathbf{0} & \Sigma_{2,k}(\mathbb{S}_{a}) \end{bmatrix} \begin{bmatrix} V_{1,k}^{H}(\mathbb{S}_{a}) \\ V_{2,k}^{H}(\mathbb{S}_{a}) \end{bmatrix}
= \mathcal{U}_{1,k}(\mathbb{S}_{a}) \Sigma_{1,k}(\mathbb{S}_{a}) V_{1,k}^{H}(\mathbb{S}_{a})
\triangleq \hat{\mathcal{U}}_{k}(\mathbb{S}_{a}) \hat{\Sigma}_{k}(\mathbb{S}_{a}) \hat{V}_{k}^{H}(\mathbb{S}_{a}).$$
(13)

where, respectively, $\mathcal{U}_k(\mathbb{S}_a)$ and $V_k(\mathbb{S}_a)$ are unitary matrix, H denotes the Hermitian transpose operation, $\Sigma_k(\mathbb{S}_a)$ is the diagonal matrix containing all the singular values of $\Delta \mathbb{Y}_{k,s}(\mathbb{S}_a)$ in the descending order, $\Sigma_{1,k}(\mathbb{S}_a)$ and $\Sigma_{2,k}(\mathbb{S}_a)$ are the partition of zero and nonzero matrices, i.e.,

$$\hat{\mathbf{\Sigma}}_{k}(\mathbb{S}_{a}) = \mathbf{\Sigma}_{1,k}(\mathbb{S}_{a}) = \operatorname{diag}\{[\sigma_{1,k}(\mathbb{S}_{a}), \cdots, \sigma_{N_{\tau},k}(\mathbb{S}_{a})]\},$$
with $\sigma_{1,k}(\mathbb{S}_{a}) \geq \sigma_{2,k}(\mathbb{S}_{a}) \cdots \geq \sigma_{N_{\tau},k}(\mathbb{S}_{a}) > 0,$
(14)

and $\hat{\mathcal{U}}_k(\mathbb{S}_a) = \mathcal{U}_{1,k}(\mathbb{S}_a)$ and $\hat{V}_k(\mathbb{S}_a) = V_{1,k}(\mathbb{S}_a)$ are partitions of $\mathcal{U}_k(\mathbb{S}_a)$ and $V_k(\mathbb{S}_a)$ according to the dimension of $\Sigma_{1,k}$ and $\Sigma_{2,k}$, respectively. Then the pseudoinverse of $\Delta \mathbb{Y}_{k,s}(\mathbb{S}_a)$ is given by

$$\Delta \mathbb{Y}_{k,s}^{\dagger}(\mathbb{S}_a) = \hat{V}_k(\mathbb{S}_a) \hat{\Sigma}_k^{-1}(\mathbb{S}_a) \hat{\mathcal{U}}_k^H(\mathbb{S}_a). \tag{15}$$

Thus, by choosing the gain matrix $\Phi_k(\mathbb{S}_a)$

$$\begin{split} & \Phi_k(\mathbb{S}_a) \triangleq \hat{\mathcal{U}}_k(\mathbb{S}_a) \phi_k(\mathbb{S}_a) \hat{\mathcal{U}}_k^H(\mathbb{S}_a), \\ & \text{with } \phi_k(\mathbb{S}_a) = \text{diag}([\rho_{k,1}(\mathbb{S}_a), \cdots, \rho_{k,p}(\mathbb{S}_a)])_{pN_q \times pN_q}, \\ & \text{and } \rho_{k,i}(\mathbb{S}_a) = \text{diag}([\rho_{k,i}(\omega_1), \cdots, \rho_{k,i}(\omega_{N_q})])_{N_q \times N_q}, \\ & \text{for } i = 1, ..., p, \end{split}$$

where $\rho_{k,i}(\omega_i) \in \mathbb{R}^+$ (\mathbb{R}^+ : the set of positive real number) is the iteration gain corresponding to $\omega_i \in \mathbb{S}_a$.

In the above DDRO-ILC algorithm, both the initialization input, $\mathbb{U}_{int}(\mathbb{S}_a)$, and the output, $\mathbb{Y}_{int}(\mathbb{S}_a)$, must have full row rank. By Eq. (9), full rank of $\mathbb{U}_{int}(\mathbb{S}_a)$ can be guaranteed by designing $U_{int,i}(\mathbb{S}_a)$ from the desired output matrix.

B. CONVERGENCE ANALYSIS

In this section, we show the convergence of the proposed DDRO-ILC technique (Objective \mathcal{O}_2). We proceed by finding a recursive form of the iterative tracking error.

Lemma 1. Let Assumptions 1 and 2 be hold, then the propagation of the active iterative tracking error is given by:

$$E_k(\mathbb{S}_a) = \beta_{k-1}(\mathbb{S}_a)E_{k-1}(\mathbb{S}_a) - \Delta D_k(\mathbb{S}_a), \qquad (17)$$

where

$$\begin{split} \boldsymbol{\beta_{k-1}}(\mathbb{S}_a) &= \boldsymbol{I} - (\Delta \mathbb{Y}_{k-1,s}(\mathbb{S}_a) - \Delta \mathbb{D}_{k-1,s}(\mathbb{S}_a)) \\ &\Delta \mathbb{Y}_{k-1,s}^{\dagger}(\mathbb{S}_a) \hat{\boldsymbol{\mathcal{U}}}_{k-1}(\mathbb{S}_a) \boldsymbol{\phi_{k-1}}(\mathbb{S}_a) \hat{\boldsymbol{\mathcal{U}}}_{k-1}^{H}(\mathbb{S}_a), \\ \Delta \boldsymbol{D}_k(\mathbb{S}_a) &= \begin{cases} \boldsymbol{D}_1(\mathbb{S}_a) - \boldsymbol{D}_{int,p}(\mathbb{S}_a), & \text{when } k = 1 \\ \boldsymbol{D}_k(\mathbb{S}_a) - \boldsymbol{D}_{k-1}(\mathbb{S}_a), & \text{when } k \geq 2 \end{cases}, \\ \text{with } \Delta \mathbb{D}_{k,s}(\mathbb{S}_a) &= \begin{bmatrix} \mathbb{D}_{int}(\mathbb{S}_a) & \Delta \boldsymbol{D}_k(\mathbb{S}_a) \end{bmatrix}_{pN_q \times ((p+1)N_q)}, \\ \mathbb{D}_{int}(\mathbb{S}_a) &= \begin{bmatrix} \boldsymbol{D}_{int,1}(\mathbb{S}_a) & \cdots & \boldsymbol{D}_{int,p}(\mathbb{S}_a) \end{bmatrix}_{pN_q \times pN_q}, \end{split}$$

$$(18)$$

In Eq. (18), $\{D_{int,i}(\mathbb{S}_a)\}_{pN_q\times N_q}$ is the output disturbance matrix during the i^{th} $(1\leq i\leq p)$ initialization process.

The proof is omitted due to space limit. It can be verified via algebraic operations.

Assumption 3. For System in Eq. (1), the following conditions are satisfied,

(1) the gain of the active system, $||\mathcal{G}(\mathbb{S}_a)||_2$, is bounded below by constants $\underline{k}_g \in \mathbb{R}^+$, respectively

$$\frac{-g}{\underline{k}_q} \le ||\mathcal{G}(\mathbb{S}_a)||_2. \tag{19}$$

(2) The output disturbance/measurement noise in all output channels are independent wide-sense stationary processes, with its 1-norm ω is bounded by a constant $\varepsilon_n \in \mathbb{R}^+$, at any given frequency ω ,

$$\sup_{\omega} ||\boldsymbol{D}(j\omega)||_1 \triangleq \sup_{\omega} \sum_{i=1}^{p} |d_i(j\omega)| \leq \varepsilon_n.$$
 (20)

(3) The size of the active initialization input, $||\mathbb{U}_{int}(\mathbb{S}_a)||_2$, is greater than a constant given by the noise to system gain ratio, i,e.,

$$k_u \triangleq ||\mathbb{U}_{int}(\mathbb{S}_a)||_2 > \frac{(\sqrt{6}+1)\varepsilon_n}{\underline{k}_g}.$$
 (21)

Remark 1. The above Assumption 3 is reasonable as for stable MIMO systems, the active system gain is bounded, and the boundaries, k_g and \underline{k}_q in Eq. (19), can be estimated through experiments. The disturbance in each output channel is bounded (Eq. (20)) and in many cases, independent from each other. Finally, the initial input shall be large enough otherwise the corresponding output, $\mathcal{G}(\mathbb{S}_a)\mathbb{U}_{int}(\mathbb{S}_a)$, would be too small—smaller than the disturbance itself—to provide useful information of the system behavior.

Lemma 2. Let Assumptions 1-3 be satisfied, then in any given k^{th} iteration,

(1) The output disturbance is bounded as

$$||\Delta \mathbb{D}_{k,s}(\mathbb{S}_a)||_2 \le \sqrt{6\varepsilon_n},$$
 (22)

and initially (i.e., k = 0)

$$||\Delta \mathbb{D}_{int}(\mathbb{S}_a)||_2 \le \varepsilon_n. \tag{23}$$

(2) The pesudo-inverse of the active output difference $\Delta \mathbb{Y}_{k.s}^{\dagger}(\mathbb{S}_a)$ is bounded above by

$$||\Delta \mathbb{Y}_{k,s}^{\dagger}(\mathbb{S}_a)||_2 < \frac{1}{k_u \underline{k}_q - \varepsilon_n}.$$
 (24)

The proof is omitted to save space. Theorem 1 (convergence condition). At any given frequency $\omega_a \in \mathbb{S}_a$, let Assumptions 1-3 be satisfied, and let the iteration gain, $\rho_{k,i}(\omega_i)$, for i=1,...,p and $j=1,...,N_q$ be chosen as,

$$0 < \rho_{k,i}(\omega_j) < \frac{2\Omega}{1+\Omega} < 2, \tag{25}$$

where $\Omega \in (1, +\infty)$ is a constant given by

$$\Omega = \frac{\underline{k}_g \times k_u - \varepsilon_n}{\sqrt{6}\varepsilon_n},\tag{26}$$

then, the DDRO-ILC algorithm converges,

$$\lim_{k\to\infty}||\boldsymbol{E}_k(\mathbb{S}_a)||_2\leq\frac{2\varepsilon_n}{1-\overline{\eta}},$$
 where $\overline{\eta}\in(0,\underline{1})$ is a constant given by

$$\overline{\eta} = \overline{\left\{ |1 - \rho_{k,i}(\omega_j)| + \frac{\rho_{k,i}(\omega_j)}{\Omega} \right\}}$$

$$\triangleq \sup_{\substack{1 \le j \le N_q \\ 1 \le i < p}} \left\{ |1 - \rho_{k,i}(\omega_j)| + \frac{\rho_{k,i}(\omega_j)}{\Omega} \right\}.$$
(28)

The proof is omitted due to space limit. C. OPTIMAL ITERATION GAIN

Corollary 1. Let the conditions in Theorem 1 be satisfied, and the iteration gain matrix is chosen as $\phi_k^*(\mathbb{S}_a) = I$, then

(1) the upper bound of the residual error is minimized, i.e.,
$$\lim_{k\to\infty}||\boldsymbol{E}_k(\mathbb{S}_a)||_2\leq \frac{2\varepsilon_n}{1-\eta^*}\leq \frac{2\varepsilon_n}{1-\overline{\eta}}, \text{ with } \quad \eta^*=\frac{1}{\Omega}, \tag{29}$$

(2) the convergence speed is maximized in the upper bound of the tracking error, i.e., $\eta^* < \overline{\eta}$ when $\phi_k(\mathbb{S}_a) \neq$ $\phi_k^*(\mathbb{S}_a)$.

The proof is omitted to save space.

IV. SIMULATION RESULTS AND DISCUSSION

In this section, we illustrate the proposed method by comparing it to the multi-axis inversion-based iterative control (MAIIC) method [2] in an output tracking example of a 3input, 3-output MIMO LTI system in simulation.

A. SYSTEM DESCRIPTION

The 3-by-3 LTI system considered is given by G(s) = $[G_{i,j}(s)] \in \mathbb{C}^{3\times 3}$ with each $G_{i,j}(s)$ being a two-pole, onezero subsystem

$$G_{ij}(s) = k_{ij} \times \frac{s + a_{ij}}{s^2 + b_{ij}s + c_{ij}},$$
 (30)

where the poles and the zeros of the subsystems $G_{i,j}(s)$ were specified by the coefficients a_{ij} , b_{ij} and c_{ij} as given by,

$$\begin{bmatrix} a_{11} & a_{12} & a_{13} \\ a_{21} & a_{22} & a_{23} \\ a_{31} & a_{32} & a_{33} \end{bmatrix} = \begin{bmatrix} 1 & 2 & 2 \\ 2 & 2 & 2 \\ 2 & 2 & 2 \end{bmatrix},$$

$$\begin{bmatrix} b_{11} & b_{12} & b_{13} \\ b_{21} & b_{22} & b_{23} \\ b_{31} & b_{32} & b_{33} \end{bmatrix} = \begin{bmatrix} 1 & 4 & 2 \\ 3 & 3 & 3 \\ 5 & 5 & 5 \end{bmatrix},$$

$$\begin{bmatrix} c_{11} & c_{12} & c_{13} \\ c_{21} & c_{22} & c_{23} \\ c_{31} & c_{32} & c_{33} \end{bmatrix} = \begin{bmatrix} 1 & 5 & 3 \\ 3 & 2 & 4 \\ 5 & 1 & 6 \end{bmatrix},$$

$$(31)$$

and the static gain coefficient $[k_{ij}] \in \mathbb{R}^{3 \times 3}$ were chosen differently for the weak- and strong- coupling system: For the weak-coupling case, $[k_{ij}] = 1$, when i = j, $[k_{ij}] =$ 0.01, when $i \neq j$, such that the convergence condition for the MAIIC algorithm [2] was satisfied, and for the strong coupling case the gain matrix $[k_{ij}]$ was chosen as the all ones matrix. i.e., $k_{ij} = 1$ for all k_{ij} s.

The frequency responses of each $G_{i,j}(s)$ for i, j = 1, 2, 3are shown in Fig. 1 for the weak- and strong- coupling case, respectively. It is clear that in the weak coupling system, the diagonal dynamics dominated in all three channels, whereas the cross-axis coupling dynamics were pronounced

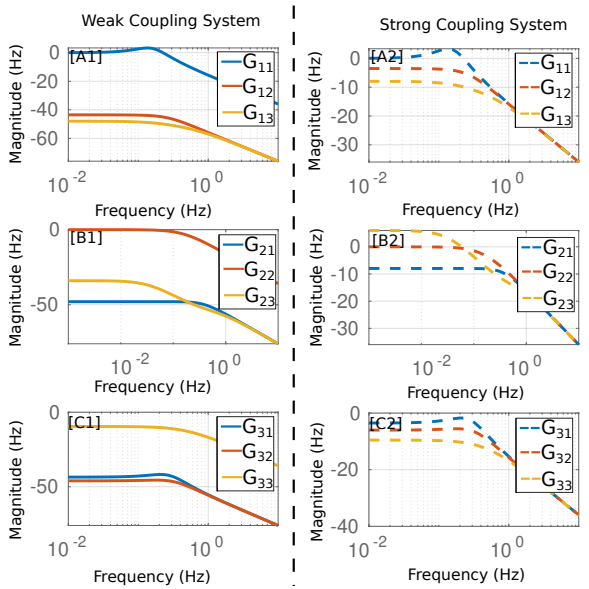
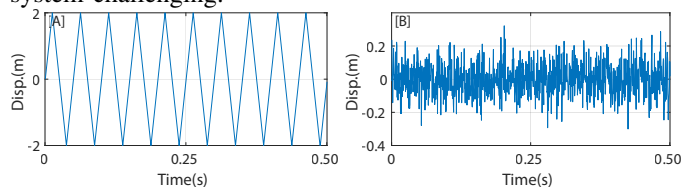


Fig. 1. [A1-C1]: Frequency response of the first, second and third input and the corresponding coupling dynamics for the weak-coupling case; [A2-C2]: Frequency response of the first, second and third input and the corresponding coupling dynamics for the strong-coupling case.

in the strong coupling case (see Fig. 1 [A2-C2]), where the off-diagonal dynamics even dominated in the second and third output channels, respectively. Such a strong cross-axis coupling dynamics made precision tracking of this MIMO system challenging



[A]: Reference 20 Hz Triangle trajectory; [B]: the output noise generated at the first output channel in the 15^{th} iteration.

During the simulation, the proposed DDRO-ILC and the MAIIC algorithms were used to generate the control inputs, respectively. As shown in Fig. 2 [A], the 20 Hz triangle wave was chosen as the desired trajectory in all three channels, and in each iteration, the output noise/disturbance was generated by the normal random numbers with zero expectation and standard deviation at 0.1. As an example, the output noise generated for the first channel in one (the 15^{th}) iteration is shown Fig. 2 [B]. The sampling time was set at 10^{-3} s.

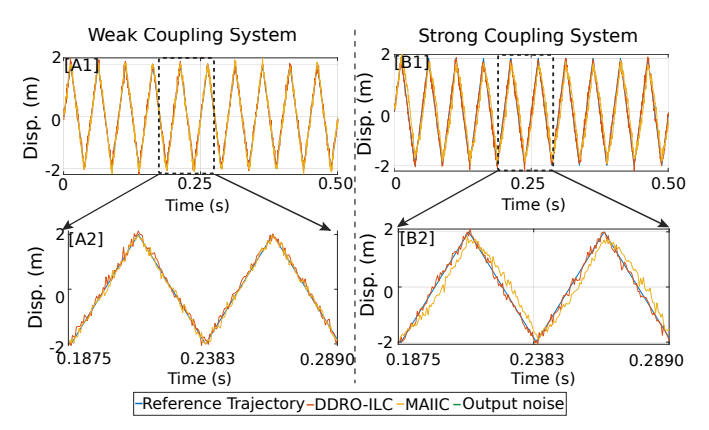
In the proposed method, the iteration gain matrix, ρ_k , was chosen as the optimal one—the identity matrix. The iteration process was terminated after 25 iterations, and the relative 2-norm error, $E_2(\%)$, was calculated in each iteration, where $E_2(\%)$ is defined as, $E_2(\%) \triangleq \frac{||y_d - y||_2}{||y_d||_2} \times 100.$

(32)

For comparison, the MAIIC method was also applied, where the iteration coefficient matrix, $\rho(s)$, was chosen as the identity matrix.

B. RESULTS AND DISCUSSION

The tracking results and the tracking error obtained by using the MAIIC method and the DDRO-ILC method after



[A1-B1]: Comparison of the tracking results of the triangle trajectory obtained by MAIIC with that by using the proposed DDRO-ILC method at the second output channel in weak and strong coupling system, respectively; [A2-B2]: The zoomed-in view of two periods in [A1], [B1],

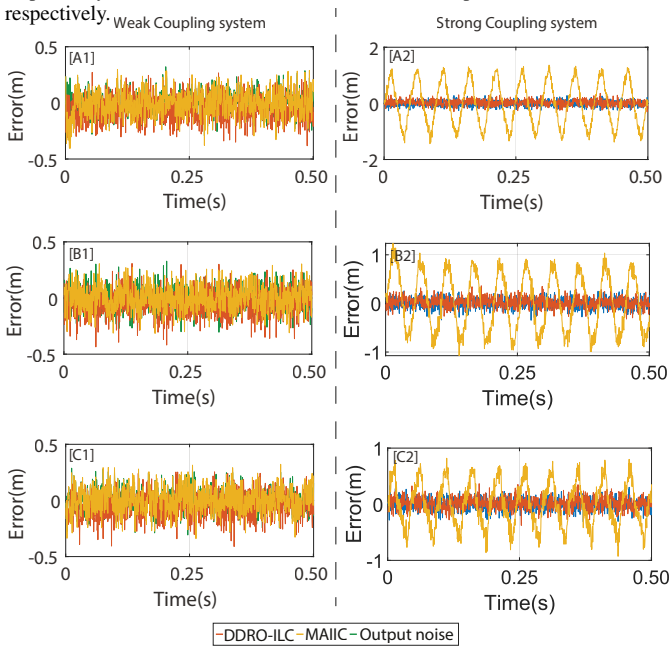


Fig. 4. [A1-C1]: Comparison of the output noise with the triangle trajectory tracking error in the weak coupling system obtained by the proposed MAIIC method and that obtained by DDRO-ILC method at first, second and third output channel, respectively; [A2-C2]: Comparison of the output noise with the triangle trajectory tracking error in the strong coupling system obtained by the proposed MAIIC method and that obtained by DDRO-ILC method at first, second and third output channel, respectively.

25 iterations are compared for both the weak and the strong coupling systems. The tracking results at the second channel are shown in Fig. 3, and the tracking error in all channels are shown in Fig. 4.

The simulation results demonstrated that the DDRO-ILC method converged rapidly and overperformed the MAIIC method. As shown in Fig. 3 [A1-A2], Fig. 4 [A1-C1] and Fig. 5 [A], for the weak coupling system tracking, both the MACIIC method and the DDRO-ILC method can track the reference triangle trajectory accurately. For example, in each channel, the tracking error was approaching the output noise level (see Fig. 3 and Fig. 4 [A1-C1]). This could also be verified by Fig. 5 [A], where the relative maximum error of the output noise, DDRO-ILC tracking error and MAIIC tracking error were all between 8% to 12% at all output channels. Therefore, the tracking results showed that when applied to the weak coupling system, both MAIIC and DDRO-ILC methods were able to overcome the crosscoupling effect and achieve precisely tracking. However, as shown in Fig. 3 [B1-B2], Fig. 4 [A2-C2] and Fig. 5 [B], for the strong coupling system, the MAIIC method was not able to track the reference trajectory since the convergence was not guaranteed due to the strong cross-coupling effect. The cross-axis coupling effect dramatically deteriorated the output performance, and the tracking error increased rapidly at all output channels (see Fig. 3 [B1-B2] and Fig. 4 [A2-C2]). But when using the DDRO-ILC method, the tracking error was still rather small. For example, when using the MAIIC method, it could not track the reference trajectories at all three output channels, and as shown in Fig. 5 [B], the relative 2-norm error, $E_2(\%)$, at these three channels were 66%, 51% and 45% . However, when using the DDRO-ILC method, $E_2(\%)$ was around 9% in all outputs, which is at least 4 time less than those in the MAIIC method, and it approaches the noise signal ratio norm (about 8.5%). Besides, as shown in Fig. 6, the proposed method converged rather quickly and reached convergence after two iterations in both weak and strong coupling systems, which was much faster than the conventional ILC methods in [8], [16]. Therefore, the experimental results demonstrated the robustness and superior performance of the DDRO-ILC method by keeping extremely low tracking error and rapid convergence at both weak and strong coupling systems.

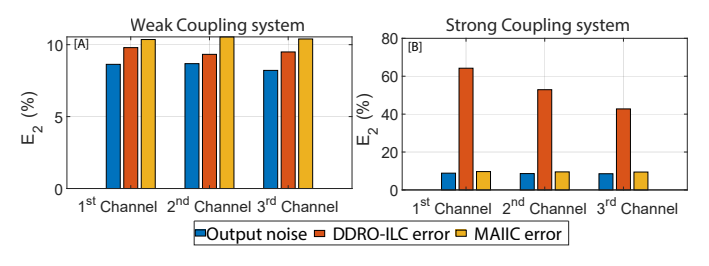


Fig. 5. Comparison of the relative 2-norm error of DDRO-ILC, MAIIC and output noise during the 25^{th} iteration at the weak coupling system [A] and the strong coupling system [B], respectively.

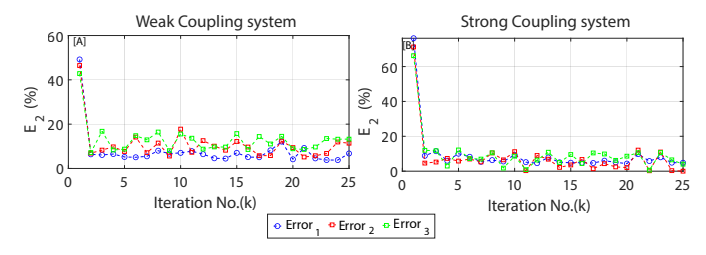


Fig. 6. Relative 2-norm error of the 1^{st} (Error₁), the 2^{nd} (Error₂) and the 3^{rd} (Error₃) channels over 25 iterations in weak [A] and strong [B] coupling systems, respectively, obtained by DDRO-ILC.

V. CONCLUSION

A data-driven iterative learning control method was proposed to achieve precisely tracking at LTI MIMO system. The convergence of the proposed method was analyzed, and

an optimal iteration gain was designed to accelerate the convergence and minimize the residual error. A numerical simulation was implemented on two LTI MIMO models with weak or strong cross-axis coupling, respectively. The simulation results showed the robustness and performance of the proposed method when compared to the MAIIC method. Future work will include enhanced computation efficiency and accuracy and extension to nonlinear MIMO systems.

REFERENCES

- [1] Ashley A Armstrong and Andrew G Alleyne. A multi-input singleoutput iterative learning control for improved material placement in extrusion-based additive manufacturing. *Control Engineering Practice*, 111:104783, 2021.
- [2] Yan Yan, Haiming Wang, and Qingze Zou. A decoupled inversion-based iterative control approach to multi-axis precision positioning: 3d nanopositioning example. *Automatica*, 48(1):167–176, 2012.
- [3] Ian Abraham and Todd D Murphey. Active learning of dynamics for data-driven control using koopman operators. *IEEE Transactions on Robotics*, 35(5):1071–1083, 2019.
- [4] Leon Liangwu Yan, Nathan Banka, Parker Owan, Walter Tony Piaskowy, Joseph L Garbini, and Santosh Devasia. MIMO ILC using complex-kernel regression and application to precision SEA robots. Automatica, 127:109550, 2021.
- [5] Lennart Blanken and Tom Oomen. Multivariable iterative learning control design procedures: From decentralized to centralized, illustrated on an industrial printer. *IEEE Transactions on Control Systems Technology*, 28(4):1534–1541, 2020.
- [6] Nic Dirkx, Jeroen van de Wijdeven, and Tom Oomen. Frequency response function identification for multivariable motion control: Optimal experiment design with element-wise constraints. *Mechatronics*, 71:102440, 2020.
- [7] Wenjie Chen and Masayoshi Tomizuka. Dual-stage iterative learning control for MIMO mismatched system with application to robots with joint elasticity. *IEEE Transactions on control systems technology*, 22(4):1350–1361, 2013.
- [8] Xiaohong Hao, Lei Zhang, and Hengjie Li. A new PD type iterative learning control in active control for vibration. In 2008 7th World Congress on Intelligent Control and Automation, pages 922–926. IEEE, 2008.
- [9] Yun-Shan Wei and Xiao-Dong Li. Varying trail lengths-based iterative learning control for linear discrete-time systems with vector relative degree. *International Journal of Systems Science*, 48(10):2146–2156, 2017
- [10] Slawomir Mandra, Krzysztof Galkowski, Andreas Rauh, Harald Aschemann, and Eric Rogers. Iterative learning control for a class of multivariable distributed systems with experimental validation. *IEEE Transactions on Control Systems Technology*, 29(3):949–960, 2020.
- [11] Jurgen van Zundert and Tom Oomen. On inversion-based approaches for feedforward and ILC. Mechatronics, 50:282–291, 2018.
- [12] Eric Gross, Masayoshi Tomizuka, and William Messner. Cancellation of discrete time unstable zeros by feedforward control. 1994.
- [13] J. Ghosh and B. Paden. A pseudoinverse-based iterative learning control. *IEEE Transactions on Automatic Control*, 47(5):831–837, 2002
- [14] Joost Bolder, Stephan Kleinendorst, and Tom Oomen. Data-driven multivariable ILC: enhanced performance by eliminating L and Q filters. *International Journal of Robust and Nonlinear Control*, 28(12):3728–3751, 2018.
- [15] Benyan Huo, Chris T Freeman, and Yanghong Liu. Data-driven gradient-based point-to-point iterative learning control for nonlinear systems. *Nonlinear Dynamics*, 102(1):269–283, 2020.
- [16] Leontine Aarnoudse and Tom Oomen. Model-free learning for massive MIMO systems: Stochastic approximation adjoint iterative learning control. *IEEE Control Systems Letters*, 5(6):1946–1951, 2020.
- [17] Wilson J Rugh. Linear system theory. Prentice-Hall, Inc., 1996.
- [18] Sigurd Skogestad and Ian Postlethwaite. *Multivariable feedback control: analysis and design*, volume 2. Citeseer, 2007.
- [19] H. K. Khalil. Nonlinear systems. Prentice-Hall, 2011.
- [20] Roger A Horn and Charles R Johnson. Matrix analysis. Cambridge university press, 2012.